The Role of Large-Scale Feedbacks in Cumulus Convection Parameter Estimation

SHAN LI

Laboratory for Climate and Ocean–Atmosphere Studies, Department of Atmospheric and Oceanic Sciences, School of Physics, Peking University, Beijing, China, and NOAA/Geophysical Fluid Dynamics Laboratory–University of Wisconsin–Madison Joint Visit Program, Princeton, New Jersey

SHAOQING ZHANG

NOAA/Geophysical Fluid Dynamics Laboratory, Princeton, New Jersey

ZHENGYU LIU

Laboratory for Climate and Ocean–Atmosphere Studies, Department of Atmospheric and Oceanic Sciences, School of Physics, Peking University, Beijing, China, and Center for Climate Research and Department of Atmospheric and Oceanic Sciences, University of Wisconsin–Madison, Madison, Wisconsin

XIAOSONG YANG

NOAA/Geophysical Fluid Dynamics Laboratory, Princeton, New Jersey, and University Corporation for Atmospheric Research, Boulder, Colorado

ANTHONY ROSATI, JEAN-CHRISTOPHE GOLAZ, AND MING ZHAO

NOAA/Geophysical Fluid Dynamics Laboratory, Princeton, New Jersey

(Manuscript received 7 February 2015, in final form 6 October 2015)

ABSTRACT

Uncertainty in cumulus convection parameterization is one of the most important causes of model climate drift through interactions between large-scale background and local convection that use empirically set parameters. Without addressing the large-scale feedback, the calibrated parameter values within a convection scheme are usually not optimal for a climate model. This study first designs a multiple-column atmospheric model that includes large-scale feedbacks for cumulus convection and then explores the role of large-scale feedbacks in cumulus convection parameter estimation using an ensemble filter. The performance of convection parameter estimation with or without the presence of large-scale feedback is examined. It is found that including large-scale feedbacks in cumulus convection parameter estimation can significantly improve the estimation quality. This is because large-scale feedbacks help transform local convection uncertainties into global climate sensitivities, and including these feedbacks enhances the statistical representation of the relationship between parameters and state variables. The results of this study provide insights for further understanding of climate drift induced from imperfect cumulus convection parameterization, which may help improve climate modeling.

1. Introduction

General circulation models (GCMs) are powerful tools to study the climate system. However, most GCMs have systematic bias in long-term simulations because of deficiencies in the representation of water and energy budgets (Gupta et al. 2013). One important cause of these deficiencies is closely related to the development of the cumulus convection parameterizations (Ma et al. 2013; Bretherton 2007). Convection parameterization can influence the performance of climate models by generating a significant fraction of the total precipitation and redistributing large-scale water vapor, thus impacting water and radiation budgets (Emanuel and Živković-Rothman 1999). Particularly in the tropics,

Corresponding author address: Shan Li, NOAA/GFDL–University of Wisconsin Joint Visit Program, Princeton University Forrestal Campus, 201 Forrestal Road, Princeton, NJ 08540.
E-mail: shan.li@noaa.gov

DOI: 10.1175/JCLI-D-15-0117.1

where convection is most active, the intensity, location, and frequency of convection can influence the structure of the Walker circulation (Park and Funk 2011; Hourdin et al. 2006; Webster and Yang 1992), the variability of El Niño–Southern Oscillation (ENSO; Webster and Yang 1992; Lau and Chan 1988; Xiang et al. 2013; Bretherton 2007), the intertropical convergence zone (ITCZ; Song and Zhang 2009), the Madden–Julian oscillation (Tokioka et al. 1988; Lin et al. 2006), and monsoon intensity (Webster and Yang 1992; Mukhopadhyay et al. 2010). Furthermore, convection can have a great impact on global climate (Tracton 1973). Although many cumulus convection parameterization schemes have been developed for decades, large uncertainties remain because of the incomplete understanding of physical processes, as well as imperfect numerical implementation. Among them, empirically set or uncertain parameter values are one major source of model biases. Cumulus convection parameters, especially those related to entrainment, have been recognized as the most important parameters that lead to the largest uncertainty in the climate projection (Rougier et al. 2009; Murphy et al. 2004).

It is known that model parameters can be estimated using observations through data assimilation approaches (Jazwinski 1970; Banks 1992a,b; Annan and Hargreaves 2004; Annan et al. 2005; Pulido and Thuburn 2006; Kang et al. 2011; Zhang 2011a; Zhang et al. 2012; Ruiz et al. 2013; Zhang et al. 2015). This data-assimilation-based parameter estimation (also known as parameter optimization) has been applied to estimate physical parameters for mitigation of parameterization mismatch (Emanuel and Živković-Rothman 1999; Aksoy et al. 2006a,b; Tong and Xue 2008a,b; Schirber et al. 2013; Ruiz and Pulido 2014; van Lier-Walqui et al. 2012, 2014; Posselt and Bishop 2012; Posselt et al. 2014). However, since convection is discontinuous in time and space (Županski 1993; Zhang et al. 2001), estimating the cumulus convection parameters is usually challenging. For example, because of its threshold nature, when there is no convection adjustment, the relationship between state variables and convection parameters represented in the model is ambiguous, which makes an accurate estimation difficult. In fact, a local convection is triggered by the large-scale environment, and the large-scale environment is in turn modified by the convection through the feedbacks between local convection and the large scales. This interaction links the "scattered" convection together and is of crucial importance to the climate system (Randall et al. 1996; Arakawa and Schubert 1974). However, most of the previous studies on convection parameter estimation are conducted in a single-column-based model (SCM) following Betts and Miller (1986), where such interaction is usually overlooked. Emanuel and Živković-Rothman (1999) tried to estimate cumulus convection parameters by minimizing model forecast errors using a variational approach based on an SCM. Golaz et al. (2007) utilized an ensemble parameter estimation technique to calibrate a single-column cloud parameterization by attempting to match predicted fields to reference large-eddy simulations. Recently, some studies used GCMs for convection parameter estimation (Schirber et al. 2013; Ruiz and Pulido 2014). For example, Schirber et al. (2013) used an ensemble Kalman filter (EnKF) to estimate convection parameters in a comprehensive GCM, in both the perfect model scenario and the real observation scenario. Both the SCM and GCM methods have advantages and disadvantages. An SCM is less expensive but does not consider large-scale feedbacks and therefore cannot fully represent the sensitivity of the climate to cumulus convection parameters (Randall et al. 1996; Emanuel and Živković-Rothman 1999). A GCM avoids these two problems, but its complexity seriously limits one's understanding on some fundamental aspects of cumulus convection parameter estimation. For example, it is difficult to isolate the cumulus convection parameter error from other error sources within a given GCM. Moreover, parameter values estimated by a GCM or an SCM may differ from each other (Schirber et al. 2013; Tiedtke 1989). On the one hand, the SCMs usually do not consider the interaction between local convection and large scales while estimating parameters while the GCMs do. On the other hand, parameters estimated with an SCM are more locally optimized, while parameters estimated with a GCM are more globally optimized. As such, when the parameter values estimated from an SCM are applied to a GCM, they could cause model biases.

In this study, to explore the role of the large-scale feedback in cumulus convection parameter estimation, a multiple-column atmospheric model is designed where the interaction between large-scale circulation and local convective columns can be easily adjusted to emulate the situation of either a GCM or an SCM. After the model description in section 2, section 3 introduces the ensemble adjustment Kalman filter (EAKF; Anderson 2001, 2003; Zhang and Anderson 2003), which is used for cumulus convection parameter estimation in this study. Experiments of cumulus convection parameter estimation with or without the large-scale feedback under different model error contexts are performed, and the results are analyzed and discussed in sections 4 and 5, respectively. Conclusions and discussions are given in section 6.

2. Model

To investigate the impact of large-scale feedbacks on cumulus convection parameter estimation, we

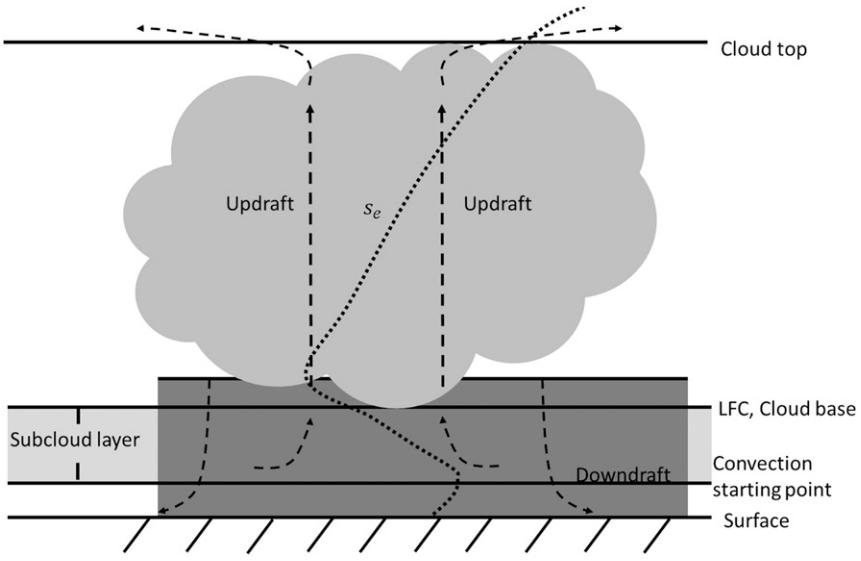

FIG. 1. Schematic figure of cloud model in SASCNV. The atmospheric column is divided into the subcloud layer and the cloud region above. In the cloud region, cumulus convection influences the environment by cumulus-induced subsidence and detrainment of saturated air. In the subcloud layer, cumulus convection affects the depth of the mixed layer through cumulus-induced subsidence. The cloud model searches for the air parcel with local maximum s_e below 700 hPa as the convection starting level. The air parcel is then taken upward to the LFC conserving s_{es}. The cloud base is the LFC. After that, the air is taken upward to the cloud top, which is defined as the height where s_{es} of the air is less than s_e of the environment. For the updraft, entrainment takes place between the starting point and the LFC, and a percentage of α of the mass flux is specified at the starting point, which is used to calculate the entrainment rate. Detrainment occurs at the cloud-top level. Downdraft happens beyond the upper level of the local minimum s_e level around 400 hPa (Pan and Wu 1995).

first design a multiple-column model based on three principles:

1) The model should be able to represent the large-scale feedback that the local convection interacts with adjoining areas. And the interaction can be easily turned on or off to simulate the fundamental feature of an SCM and a GCM so that we can show the difference between SCM parameter estimation and GCM parameter estimation.
2) The model should be able to drive the cumulus convection parameterization scheme and should include important physical rules, such as convection–radiation equilibrium and convection driven by warm sea surface temperature (SST).
3) The model should be simple enough so that it is easy to perform parameter estimation with an ensemble method and the sources of model errors are easily isolated.

The model is designed to simulate typical conditions in the tropical Pacific region, especially the Walker circulation area, consisting of regions with high convective activity and regions with low convective activity. The model contains 10 columns, with a cyclic boundary condition, and 28 vertical sigma levels. The surface pressure is fixed at 1000 hPa, and the top model layer is about 2.7 hPa. The prognostic equations are as follows:

$$\frac{\partial T}{\partial t} = -u(z)\frac{\partial T}{\partial x} + g\frac{\partial H}{\partial p} + F_T + R \quad \text{and} \tag{1}$$

$$\frac{\partial q}{\partial t} = -u(z)\frac{\partial q}{\partial x} + g\frac{\partial E}{\partial p} + F_q, \tag{2}$$

where T and q are temperature and specific humidity. This model is a simple radiative–convective equilibrium model with large-scale advection.

The convective adjustment terms, F_T and F_q, are calculated using the simplified Arakawa–Schubert convection parameterization scheme (SASCNV; Pan and Wu 1995; see http://www.nco.ncep.noaa.gov/pmb/codes//nwprod/ngac.v1.0.0/sorc/ngac_fcst.fd/atmos/phys/sascnv.f). This cumulus convection parameterization scheme is a one-type cloud scheme simplified from the Arakawa–Schubert scheme (Arakawa and Schubert 1974; Lord and Arakawa 1980; Lord 1982; Grell 1993). SASCNV includes three parts: static control, dynamic control, and feedbacks. In static control, a cloud model is used to describe thermodynamic properties of the updraft and downdraft (Fig. 1). For the updraft, in each column, the

TABLE 1. Tunable parameters in SASCNV.

Symbol	Description	Default value	Valid range
M_b (Pan and Wu 1995; Arakawa and Schubert 1974)	The integration time for unit mass flux	10.00 s	0 s to 1.5 min
E_d (Sui et al. 2007; Braham 1952)	Maximum precipitation efficiency	0.30	0 to 1
α (Pan and Wu 1995; Schirber et al. 2013; Klocke et al. 2011)	A constant in the calculation of the entrainment rate	0.50	0 to 1
E_v (Mrowiec et al. 2012)	Evaporation efficiency	0.07	0 to 1

convection starts at the level of local maximum of moist static energy s_e. An air parcel from this level is lifted to find the level of free convection (LFC), which defines the cloud base. The level where the saturation moist static energy s_{es} of the lifted air parcel is smaller than s_e of the environment is defined as the cloud top. Assuming that entrainment only occurs between the convection starting point and cloud base, the parcel mass flux is rederived (Pan and Wu 1995). A portion of α of the mass is specified at the starting point, which helps calculate the entrainment rate. Detrainment occurs at the cloud top. The downdraft starts at the upper level of local minimum s_e. In the dynamic control, the mass flux is determined by assuming a balance between the generation of moist convective instability by large-scale processes and its destruction by cumulus convection. The feedback of the cumulus onto the large-scale environment variables T and q is calculated using the mass flux function (Pan and Wu 1995). There are five tunable parameters that have great impact on the SASCNV parameterization (Pan and Wu 1995). Four of them are chosen for estimation (Table 1). The integration time scale for a unit mass flux M_b is used to calculate the balance between the destabilization of an air column by large-scale atmosphere and the stabilization of the cumulus convection (Pan and Wu 1995; Arakawa and Schubert 1974). The maximum precipitation efficiency E_d affects the water budget. The percentage of entrained mass originating at the starting point α is used to calculate the entrainment rate and has been used for parameter estimation in previous studies (Schirber et al. 2013). This parameter is considered to be very important for the estimation of the uncertainty of climate sensitivity (Murphy et al. 2004; Schirber et al. 2013; Klocke et al. 2011; Knight et al. 2007). The evaporation efficiency E_v is closely related to water vapor distribution. The other unselected parameter is a constant to calculate detrainment rate β. Similar to the entrainment parameter α that controls the updraft mass flux, β controls the downdraft mass flux. The net updraft mass flux is therefore the residual of the two mass fluxes. Since the updraft process is much more dominant, the influence of this detrainment parameter is relatively small. The sensitivity of model states to this parameter is the smallest among all five tunable parameters (not shown). Therefore, it is difficult for the uncertainty of this parameter to be transferred to the observable model states, making it not very suitable for parameter estimation with statistical method. Special treatment is needed to enhance the signal-to-noise ratio in the parameter estimation process. It takes a much longer time for estimated β to converge to the truth; therefore, it is not currently considered in this work. Table 1 lists the default values of the chosen parameters that have been used for medium-range forecasts by the National Centers for Environmental Prediction since the late 1990s (Pan and Wu 1995).

The first term on the right-hand side of Eqs. (1) and (2) is advection, where u is the horizontal wind as a function of height z. The horizontal wind and vertical velocity are fixed as constant profiles given by the time mean and space mean from the output of an atmospheric general circulation model in the tropical Pacific (10°S–10°N, 120°E–90°W) during 1979–2011. The distance ∂x in this term is set to be about 400 km. In most cumulus parameterization studies, this advection term, reflecting the interaction between large scales and local convection, is smaller than the convection adjustment term and is usually prescribed with observations in SCM-based studies (Randall et al. 1996; Emanuel and Živković-Rothman 1999) so that the local convection impacts only itself and does not interact with the large-scale flow. In our study, the large scale is turned off by prescribing the neighboring information needed in the advection term; therefore, the local convection does not interact with other locations through temperature and moisture gradient. However, recent studies show that the advection, especially the midlevel moisture advection, can greatly influence the performance of the deep convection parameterization and is therefore very important (Sobel and Bellon 2009; Bretherton 2007). In the real world, the large-scale feedback can be very complicated. For example, the local convection can influence the heat and water budget of the mean flow through radiation, wind, and pressure adjustment. These influences on the large-scale flows on the one hand are transferred to other locations and on the other hand impact the local atmospheric stability in the future. In our study, because of its simplicity, the advection term is used as a representation

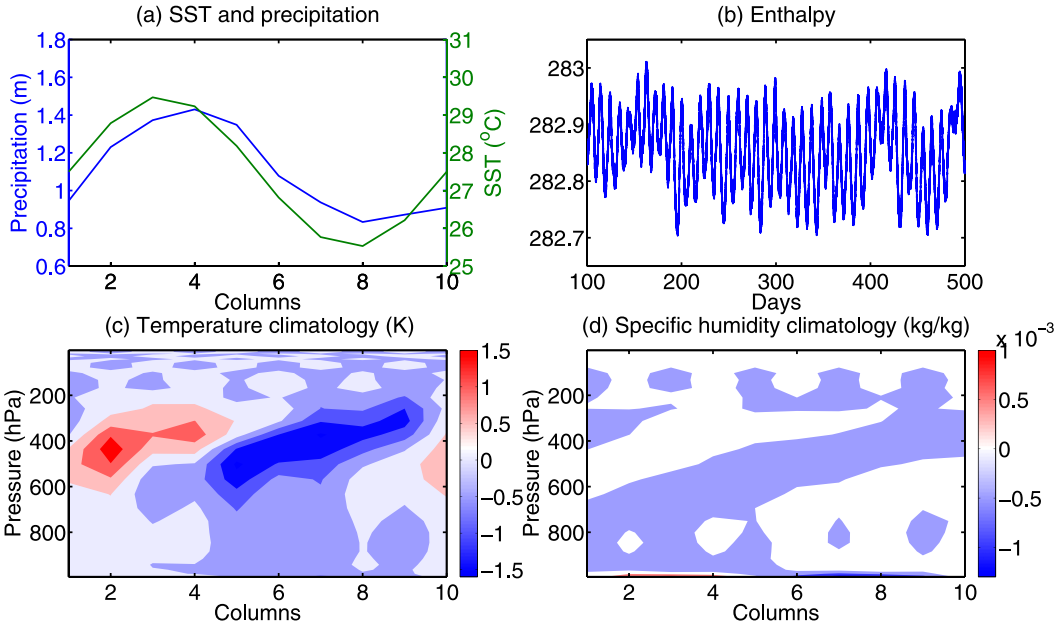

FIG. 2. Model performance. (a) Fixed model boundary sine curve for SST (dark green line) and accumulated precipitation (blue line) for 10 000 time steps after spinup along 10 columns and (b) the evolution of total enthalpy after spinup. The calculation of enthalpy follows that of Emanuel and Živković-Rothman (1999). Spatial distribution of model (c) temperature and (d) moisture climatology departures with respect to spatial average.

of the interaction in order to make the physical question clear and focused.

The second terms of Eqs. (1) and (2) are the turbulent heat and moisture flux adjustment ($g\partial H/\partial p$ and $g\partial H/\partial p$, respectively), where

$$H = \rho^2 g k_\theta \frac{\partial \theta}{\partial p} \quad \text{and} \tag{3}$$

$$E = \rho^2 g k_q \frac{\partial q}{\partial p} \tag{4}$$

(Rennó et al. 1994). The variables H and E are heat and moisture fluxes; g is the gravitational acceleration; ρ is the air density; p is the air pressure; θ is the potential temperature; and k_θ and k_q are vertical diffusion coefficients for temperature and moisture equal to $2\,\mathrm{m^2\,s^{-1}}$. In the boundary layer, heat and moisture fluxes are calculated using the following aerodynamic equations [Eqs. (5) and (6)] (Fairall et al. 1996; Fairall and Bradley 2003; Liu et al. 1979) with a "swamp" ocean surface, following Rennó et al. (1994):

$$H = \rho c_p c_h |v|(\theta_s - \theta_a) \quad \text{and} \tag{5}$$

$$E = \rho c_d |v|(q_s - q_a), \tag{6}$$

where c_p is the air heat capacity. The transfer coefficient for heat c_h is equal to 0.0012, and that for moisture c_d is equal to 0.0025. The surface potential temperature calculated with SST is θ_s, and the surface specific humidity calculated as the saturate specific humidity given SST is q_s. The potential temperature and specific humidity calculated from the temperature and humidity at the lowest model level averaged over last 24 h for numerical stability are θ_a and q_a (Rennó et al. 1994). The SST distribution is fixed as a sine curve along 10 columns (dark green line, Fig. 2a). The wind speed at the surface along the direction of the cyclic boundary domain $|v|$ is fixed at $5\,\mathrm{m\,s^{-1}}$, as in Rennó et al. (1994). The surface pressure is fixed at 1000 hPa.

The radiative cooling rate of the atmosphere is R in the temperature tendency equation. Following the method of Emanuel and Živković-Rothman (1999), it is assumed that the radiative cooling of the atmosphere is uniformly distributed in the atmosphere below 100 hPa, with a value of $-2\,\mathrm{K\,day^{-1}}$ in our study. Between the 100-hPa level and the model top, R equals zero.

The initial conditions for the temperature and moisture are obtained after a spinup of 10^5 time steps starting from the climatology of the averagely distributed 10 columns across the tropical Pacific during 1979–2011 from the output of an atmospheric circulation model. The time stepping is a leapfrog scheme, with an Asselin (1972) filter to mitigate the computational instability. The time integration step size is 15 min. The spatial difference scheme for advection is a center difference scheme. The model conserves enthalpy well after the

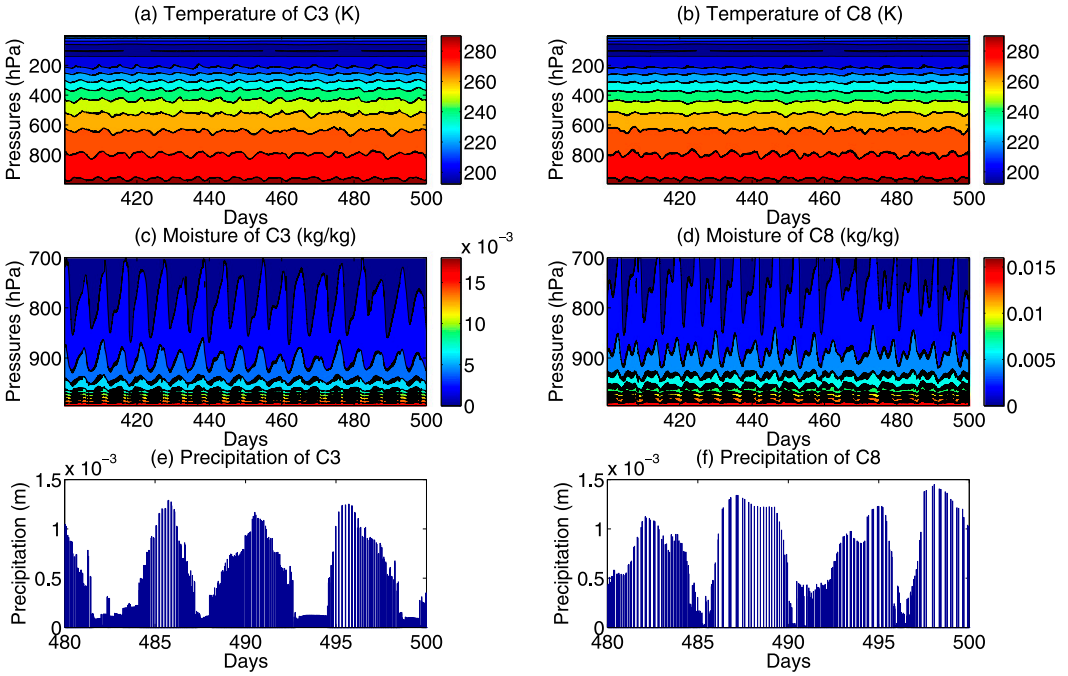

FIG. 3. Time evolution of modeled (a) temperature, (c) moisture profiles, and (e) precipitation of column 3 (convectively active column) and (b),(d),(f) column 8 (convectively inactive column).

spinup (Fig. 2b). The spatial pattern of the model climatology can be seen in Figs. 2c and 2d. The precipitation pattern (Fig. 2a, blue line), which indicates the convection distribution, is strongly influenced by the SST, with a peak at columns 3 and 4 and a valley at columns 8 and 9. Because of the presence of advection and vertical wind shear, the peak and valley of precipitation shift slightly eastward of those of SST.

Under the influence of the radiative cooling, convective adjustment, boundary heating, and constant wind shear, the model displays a 7-day oscillation that can be found in the time evolution of enthalpy (Fig. 2b), temperature and moisture profiles (Figs. 3a–d), and precipitation (Figs. 3e,f). The convection happens intermittently and is more frequent in convectively active regions (columns 2–4) and less frequent in convectively inactive regions (columns 7–9).

This 10-column radiative–convective equilibrium model, with a time scale of about 7 days, is able to represent the convection process in the atmosphere in the tropics. The advection term serves as a simple interaction between convection processes and the large-scale motion. Within this simple conceptual model, we are able to study the influence of large-scale feedbacks in cumulus convection parameter estimation with an ensemble-based method. An SCM-like method and a GCM-like method are used to drive the cumulus convection parameterization and perform parameter estimation. The main difference between the two is whether there are interactions between large-scale backgrounds and individual convection; that is, whether the individual convection has an influence on the large-scale pattern and the large-scale pattern in turn exerts feedbacks on the individual convection (Randall et al. 1996). In this study, we use the 10-column convection model linked by advection to simulate a simplified general circulation model (SGCM). When the feedback between the convective column and the large scales is turned off by prescribing the surrounding information with observations in the advection terms, the model degenerates to a simplified single-column model (SSCM). The experiment is designed under the twin-experiment framework. The SGCM with default parameter values is first integrated to obtain a long time series as the "truth." Then the "observations" of temperature and moisture are created by adding random Gaussian-distributed errors onto the truth. The observational error for temperature and moisture are 0.01 K and $1 \times 10^{-5}\,\mathrm{kg\,kg^{-1}}$ (10% of the variance of temperature and moisture), respectively. After that, two model configurations, the SGCM and SSCM with biased parameter values, are used for parameter estimation experiments and are compared with each other. For SSCM, we test two columns: a convectively active column (column 3, called $\mathrm{SSCM_{C3}}$; Table 2) and a convectively inactive column (column 8, called $\mathrm{SSCM_{C8}}$; Table 2). The integration of SSCM is

TABLE 2. Model configurations and observation systems.

	Large-scale feedbacks	Modeled column	Observations
SGCM	On	10 columns	10 columns
$SGCM_{C3}$	On	10 columns	Columns 2, 3, and 4
$SGCM_{C8}$	On	10 columns	Columns 7, 8, and 9
$SSCM_{C3}$	Off	Column 3	Columns 2, 3, and 4
$SSCM_{C8}$	Off	Column 8	Columns 7, 8, and 9

computed using Eqs. (1)–(6) as well. During the integration, the turbulent flux term, convection term, and radiation term can be calculated within the column itself, while only the advection term requires temperature and moisture information from neighboring columns. The prerecorded observations of the neighboring columns (columns 2 and 4 for $SSCM_{C3}$ or columns 7 and 9 for $SSCM_{C8}$) are used to compute the advection term for the model column (column 3 or column 8). This SSCM method is used by many studies to optimize the parameters in a cloud parameterization scheme (Emanuel and Živković-Rothman 1999; Golaz et al. 2007). In this SSCM configuration, two different columns (column 3 for $SSCM_{C3}$ and column 8 for $SSCM_{C8}$) are used to illustrate the scattered nature of convection: in reality, there are observations located in convectively active regions, such as the tropical western Pacific warm pool, and there are also observations located in convectively inactive regions, such as the cold tongue area in the tropical eastern Pacific. Are observations in convectively inactive regions of any help for estimating cumulus convection parameters? With such observations, what is the performance of an SCM and a GCM in estimating convection parameters?

3. An ensemble Kalman filter for parameter estimation

The EAKF (Anderson 2001, 2003; Zhang and Anderson 2003) is used for data assimilation and parameter estimation in this study. The EAKF maintains nonlinearity of the background flow by adjusting the ensemble mean and anomaly separately (see Anderson 2001, 2003, 2010; Zhang and Anderson 2003; Zhang et al. 2007; Wu et al. 2013) through a two-step adjustment (Anderson 2003; Zhang and Anderson 2003; Zhang et al. 2007). The first step computes the observational increment Δy^o. The second step projects the observational increment onto model states and parameters being estimated through a linear regression:

$$\Delta x^u_{l,i} = \frac{\mathrm{cov}(\Delta x^p_l, \Delta y^a_k)}{\sigma^{a2}_k} \Delta y^o_{k,i} \quad \text{and} \tag{7}$$

$$\Delta \varphi^u_{m,i} = \frac{\mathrm{cov}(\Delta \varphi^p_m, \Delta y^a_k)}{\sigma^{a2}_k} \Delta y^o_{k,i}, \tag{8}$$

where $\Delta y^o_{k,i}$ is the observational increment at the kth observational location for the ith ensemble member. The error covariance between the background ensemble of the lth state variable and the analysis ensemble for the observation at the kth observational location is $\mathrm{cov}(\Delta x^p_l, \Delta y^a_k)$. The error covariance between the background ensemble of the mth parameter and the analysis ensemble for the observation at the kth observational location is $\mathrm{cov}(\Delta \varphi^p_m, \Delta y^a_k)$. The standard deviation of the model state ensemble at the location k is σ^a_k. Note that the relationship between convection and cloud-related parameters and observable model variables could be complicated and highly nonlinear (Schirber et al. 2013; van Lier-Walqui et al. 2012). Most ensemble Kalman filter techniques are based on a linear approximation assumption (Anderson 2001, 2003, 2010) that a small error is growing linearly within a short time period. Therefore, with a linear approximation in the EAKF, if the error covariance $\mathrm{cov}(\Delta \varphi^p_m, \Delta y^a_k)$ estimated by the ensemble is not accurate, it would likely lead to unreliable estimation of the parameters.

In addition, a spatial average update scheme is used (Aksoy et al. 2006a,b) in our study to avoid when too many observations are used to estimate a single-parameter value, the sampling error will accumulate, which leads to a noisy estimation. In the parameter estimation process, each observation generates a parameter increment $\Delta\varphi$, and the averages of these parameter increments from all observations are averaged to get a final parameter increment. This final parameter increment is then added on the prior parameter ensemble to get a posterior parameter ensemble. And this posterior parameter ensemble is conveyed to the model and used to integrate the model.

In our experiment, the ensemble size is 20. The EAKF prefers small ensemble size because, first, the EAKF is able to provide accurate estimation with small ensemble size (Anderson 2001, 2003, 2010), and second, when a large ensemble is used, an outlier behavior may occur (Anderson 2010). We repeated parameter estimation for larger ensemble sizes; no significant improvement was found. And 20 is an ensemble size generally affordable for many models. The data assimilation and parameter estimation interval is every 25 model time

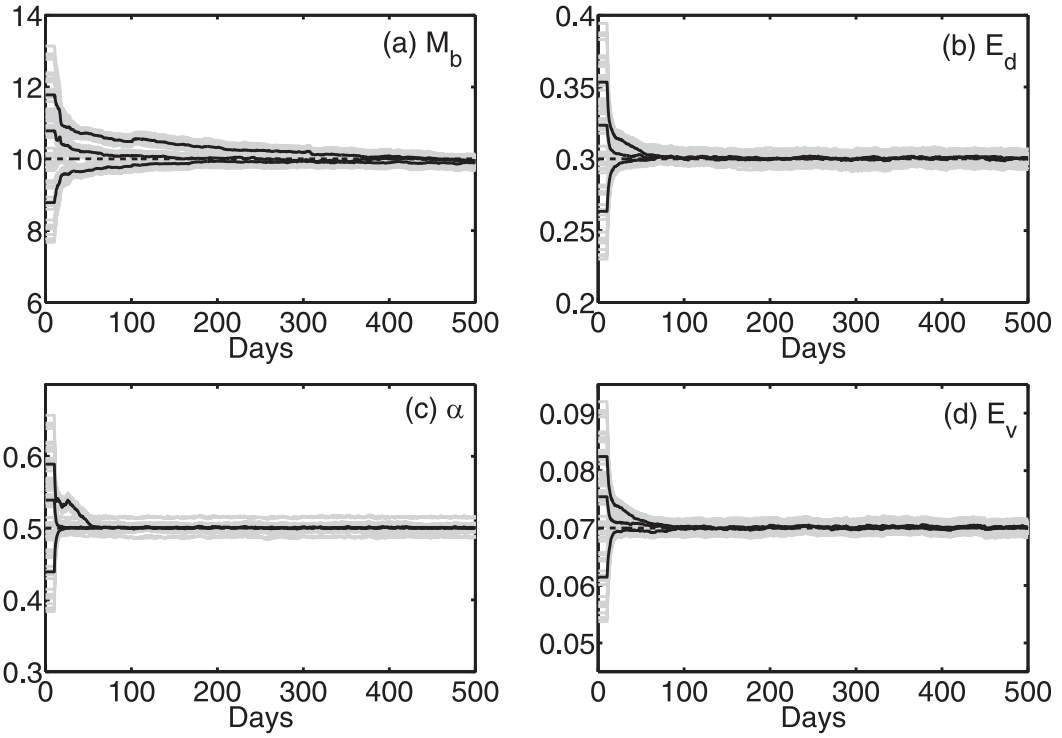

FIG. 4. Single-parameter estimation in perfect SGCM. In the perfect SGCM, the model is the same as the truth model, except for one biased parameter. The results of four parameters in SASCNV: (a) M_b, (b) E_d, (c) α, and (d) E_v. Dashed black lines are default (truth) values of the parameters. Solid black lines represent ensemble mean of the estimated parameter. For each parameter, three estimation experiments are conducted with three different initial parameter biases (10%, −10%, and 20% of the default values) to validate the robustness of parameter estimation. Solid gray lines indicate the ensemble members.

steps (~6 h). Parameter estimation is carried out after 1000 model time steps, when the state estimation has reached quasi equilibrium (Zhang et al. 2012; Wu et al. 2013). It is noted that, for a bounded model state variable (e.g., humidity q) the probability often exhibits non-Gaussian distributions because of the lower bound. Many studies apply forms of transformation (Schirber et al. 2013; Hu et al. 2010) to mitigate this problem. In our study, when the humidity falls below zero, it will be pulled back to zero. In addition, the estimated parameters also have a physically meaningful threshold (listed in Table 1). When the estimated parameters exceed the threshold, they are pulled back to the threshold values.

The complete observation system generated from the "truth model" simulation contains independent observations of temperature and moisture for 28 levels and 10 columns. In the following experiments, we first use the complete observation system to conduct an SGCM experiment (row 1 of Table 2). Then we use the observations in convectively active (or inactive) regions to conduct another four experiments with two model configurations (SSCM and SGCM) and two observation systems (denoted with subscripts C3 and C8) to form impartial comparisons (rows 2–5 of Table 2). The parameter estimation results are denoted by SSCM_{C3} and SGCM_{C3} (SSCM_{C8} and SGCM_{C8}).

4. Parameter estimation in a perfect-model context

a. Single-parameter estimation

In this section, five single-parameter estimation experiments are carried out with different configurations: the SGCM, SGCM_{C3}, SGCM_{C8}, SSCM_{C3}, and SSCM_{C8} (Table 2). We first present the results of the single-parameter estimation in the SGCM serving as a proof-of-concept study. The SGCM model is the same as the truth model (with all 10 columns), except for one erroneously set parameter to be estimated. For the single-parameter estimation, an initial parameter bias (e.g., $\Delta\alpha$) is added to the default (truth) value α_{truth} to create the erroneously set parameter. In our experiment, we tried three cases, $\Delta\alpha = 10\%$, -10%, and $20\% \times \alpha_{\text{truth}}$ (corresponding to different parameter ensemble starting points in Fig. 4) to emulate different parameter initial biases. The other three parameters remain at their default values. This emulates a simple deficient general

climate model case in which only one parameter is erroneously set. To represent the probability distribution of the truth parameter value, a parameter ensemble is created by perturbing the biased α_0 with a Gaussian distribution of $N(0, 10\% \times \alpha_{\text{truth}})$. The model is then integrated with this parameter ensemble. It is noted that the uncertainty of each parameter is different. A small bias and a small perturbation of $10\% \times \alpha_{\text{truth}}$ help ensure that the parameter ensemble members do not go beyond the physical range.

First, in SGCM, a perfect observation system of all temperature and moisture observations of 10 columns and 28 levels is used to conduct an idealized parameter estimation experiment. Parameter estimation can successfully retrieve the truth values of all the four parameters (Fig. 4) from different initial guesses. It seems that, for parameters E_d, α, and E_v, the relationships between parameters and state variables are relatively more robust, and they converge to the truth more quickly (Figs. 4b–d). For parameter M_b, the convergence takes a longer time (Fig. 4a). This is because M_b influences temperature and moisture more indirectly, and its relationship with state variables is weaker than that of other parameters so that the model's response to this parameter is weaker, which makes the parameter estimation noisier. In SASCNV, the stabilization effect of a unit cloud mass flux during a short time M_b is first calculated. By forming the ''large-scale destabilization and cloud stabilization'' quasi equilibrium, the total mass flux is calculated. The total mass flux is then used to calculate the feedback of the cloud on temperature and moisture. Therefore, the relationship between M_b and model states is more an indirect accumulation process. In ensemble parameter estimation, it takes longer for the parameter–state relationship to set up. In conclusion, through the EAKF, a biased parameter in a perfect-model context can be corrected by assimilating observations into the model and by estimating the parameter by making full use of the relationship between the parameter and state variables.

After validating the robustness of the EAKF in parameter estimation, we compare the results of SGCM and SSCM under the perfect model framework to study the role of feedbacks between large-scale motion and local convection in cumulus convection parameter estimation. In SGCM_{C3} (or SGCM_{C8}), the model is the same as the truth model, except for a single erroneously set parameter. The large-scale feedback is turned on by allowing interactions between different columns through advection. The observations of convectively active (inactive) columns, columns 2–4 (7–9), are used for data assimilation and parameter estimation. This SGCM setting is to emulate a general circulation model where the large-scale feedback between local convection is allowed. In contrast, the SSCM_{C3} and SSCM_{C8} are used to emulate the SCM setting where only one single column is used for model integration, and the information of the neighboring columns are needed to calculate the temperature and moisture gradients in the advections term is prescribed with observations. Under this circumstance, the local convection only affects the local column itself, without having any feedbacks with other columns. In SSCM_{C3} (SSCM_{C8}), the model column locates at column 3 (8), where convection is more (less) active (Fig. 2a). Observations of column 2 (7) and column 4 (9) are used to prescribe surrounding information in the advection terms for column 3 (8), and the observations of column 3 (8) are used for data assimilation and parameter estimation. In the SSCM configuration, the large-scale information is prescribed by observations, which means that the interaction between large scales and local convection is turned off (Table 2). In reality, to validate the cumulus convection parameterization scheme, a modeler usually uses an SCM and abundant observational data from a certain observation program located at an intensive convection region. Here, two kinds of observations systems (located at convectively active or inactive regions) are used in our experiments in this section in an attempt to answer the following question: If the observation program is located at a convectively inactive region, can it be used for cumulus convection parameter estimation? Figure 5 shows the results of estimation for four parameters in the SGCM_{C3}, SGCM_{C8}, SSCM_{C3}, and SSCM_{C8}.

Generally, for each observation system, the estimation in the SGCM (red and pink lines) is more accurate and signal dominant than that in the SSCM (blue and cyan lines), although some of the estimations in the SSCM_{C3} (blue lines) are also satisfying under this framework (Fig. 5). Estimated parameters E_d, α, and E_v in the SSCM_{C3} and SSCM_{C8} have larger biases. This is because turning off the large-scale feedback leads to a damping effect on the parameter perturbation, which results in an underestimate of the model sensitivity to the parameter. In the ensemble method, each ensemble member has its perturbed parameter value. In the SGCM_{C3} and SGCM_{C8}, the ensemble spread for each column represents two kinds of sensitivities (or uncertainties) induced by this parameter uncertainty. The first is local sensitivity of the local state variables as a response to the parameter uncertainty, including the sensitivities of the heat/moisture flux term, and the convective adjustment term. The second is the sensitivity induced by the large-scale feedback represented by the advection term. This second kind of sensitivity includes two parts. One is the advected sensitivities from

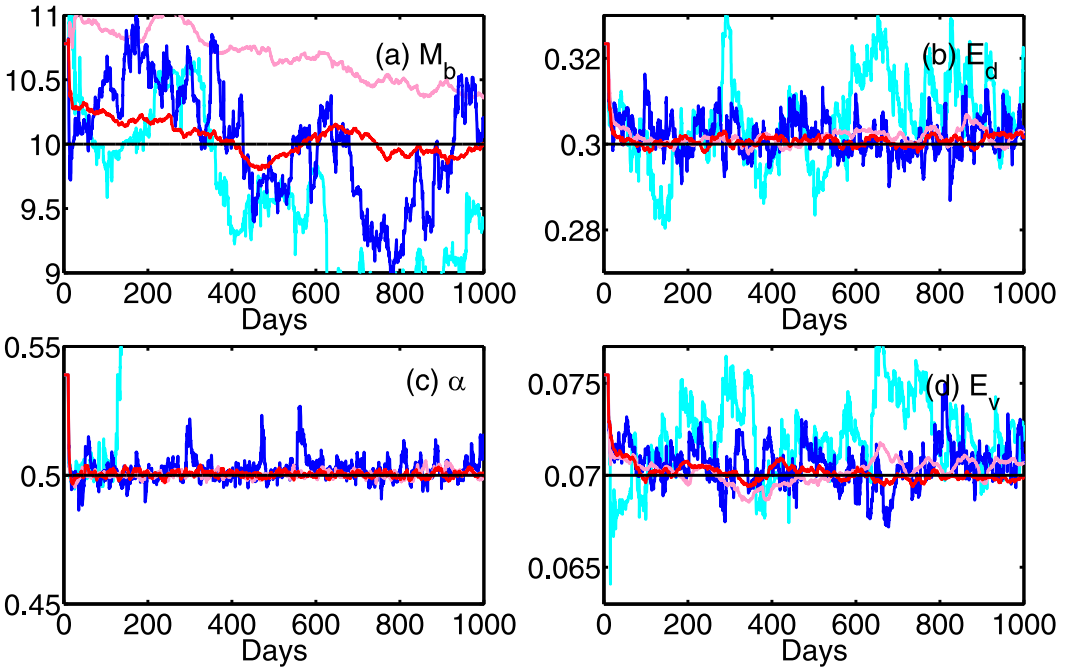

FIG. 5. Ensemble means of estimated values for parameter (a) M_b, (b) E_d, (c) α, and (d) E_v through the $SGCM_{C3}$ (red lines), $SGCM_{C8}$ (pink lines), $SSCM_{C3}$ (blue lines), and $SSCM_{C8}$ (cyan lines). The truth values of these parameters are marked as black lines.

neighboring columns; the other is the sensitivity that was projected from local column to neighboring column in an earlier time and projected back to local column through advection at the current time. In the SGCM, where large-scale feedbacks are turned on, every column is affected by this parameter perturbation, and the model states respond to the perturbation according to the model physics. However, in the SSCM, where large-scale feedbacks are turned off, only the modeled column is affected by the parameter perturbation, while the surrounding columns are prescribed with observations from the truth model with the default parameter value. Under this circumstance, the uncertainty caused by the parameter perturbation in the modeled column is damped through advection. The two parts of the large-scale feedback sensitivity are both removed. The spread of the ensemble in the SSCM therefore underestimates the model sensitivity to cumulus convection parameters. And the ensemble-evaluated covariance between cumulus convection parameters and state variables becomes less robust. This sensitivity underestimation can be examined through a parameter sensitivity study. For doing that, a 20-member ensemble is formed by perturbing each parameter with random noise from a Gaussian distribution of a zero mean and a variance equal to 10% of the default parameter value. This ensemble is integrated from the same initial condition without doing data assimilation and parameter estimation. The standard deviation (SD) of the state variables is used to represent the sensitivity because, with the same initial conditions, the deviation of evolving ensemble members is caused by merely parameter differences (Liu et al. 2014a,b). Figure 6 shows the mean SD evolution of temperature for columns 3 and 8 in the SGCM (red and pink lines), $SSCM_{C3}$ (blue lines), and $SSCM_{C8}$ (cyan lines) with perturbed parameters (moisture has similar behavior but less pronounced than temperature). It is seen that α is the most sensitive parameter, with the highest SD (Fig. 6c), while other parameters have lower sensitivities. Most of the time, the SDs of $SSCM_{C3}$ and $SSCM_{C8}$ are smaller than that of SGCM. For the most sensitive parameter α, the SD of $SSCM_{C3}$ is almost comparable with that of SGCM, which contributes to a relatively good estimate of α in $SSCM_{C3}$ (Fig. 5c). It is noted that it is highly likely that one parameter has different sensitivity for different values with itself and other parameters. However, it is assumed that a 10% variation around its default value still keeps the parameter far away from the critical value beyond which the sensitivity of both itself and other parameters can be significantly different.

The parameter sensitivity also displays a 7-day oscillation (Fig. 5), which is the result of the 7-day oscillation of the model states. The precipitation peaks about every 7 days, indicating strong atmospheric instability and large convective adjustment. In our model and most GCMs, the convection parameters take effect through

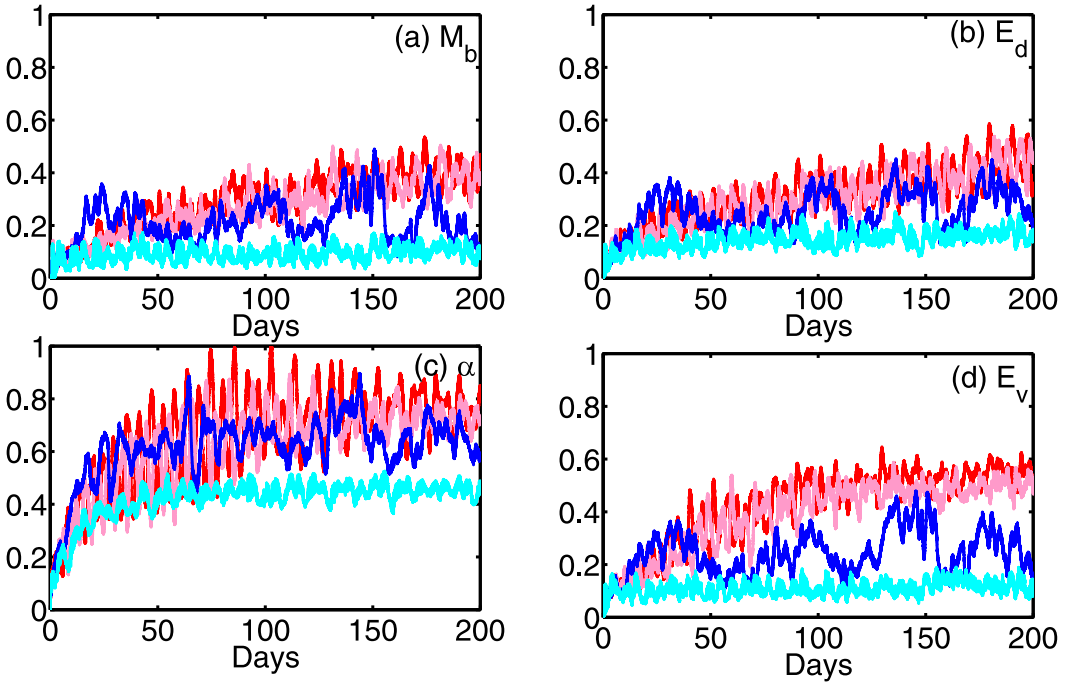

FIG. 6. The SD of the SGCM (red for column 3 and pink lines for column 8), $SSCM_{C3}$ (blue lines), and $SSCM_{C8}$ (cyan lines) to cumulus convection parameters.

convective adjustment. Large convective adjustment helps transfer the parameter uncertainty into the large spread of model states, which results in large model sensitivity to the parameter. In convectively active regions, there is more convection, which more efficiently transfers the parameter uncertainty into that of model states, which later provides more signal in estimating the parameter–state covariance.

In our simple multiple-column model, the large-scale feedback only takes effect through the temperature and moisture advection term. However, in reality, the form of large-scale feedbacks could be very complicated. The perturbation of the cumulus convection parameters not only affects the local temperature and moisture, but it also affects other columns and modifies the large-scale temperature and wind fields, which in turn reconciles the local vertical motion and influences the stability of the local column in the future. In most SCM configuration parameter estimation experiments, the sensitivities associated with these large-scale feedbacks are usually not considered.

Parameter estimations using observations of convectively active regions are more accurate and stable than those using observations of convectively inactive regions for both the SSCM and SGCM. And this is even more crucial to parameter estimation with the SSCM. This is because the model column in $SSCM_{C8}$ is located at column 8, where there is less convection (Fig. 2a) as a result of unfavorable SST. During model integration, there are more time steps with no convection in ensemble members or in observations. This has two consequences. First, with less convection, the model has fewer opportunities to build up the relationship between the cumulus convection parameters and state variables, and the parameter sensitivity is further underestimated (Fig. 6). Second, there would be more occasions where no-convection observations are used to update ensemble states and parameters, and convection observations are used to update no-convection ensemble states and parameters. Neither update is reasonable because the error covariance represented by the ensemble is not well defined. Therefore, estimation in $SSCM_{C8}$ further drifts away from the truth value (Figs. 5a,c, cyan lines). However, because of the large-scale linkage, with only observations of convectively inactive regions, the $SGCM_{C8}$ can sometimes provide even better estimation than $SSCM_{C3}$ (Figs. 4b,c).

Figure 7 serves as a concrete example of how the large-scale feedback impacts the model response to parameter perturbation (parameter sensitivity) so as to contribute to more signal during parameter estimation. In Fig. 7, the experiment setting is exactly the same as that of Fig. 6c. The parameter α is perturbed into a 20-member ensemble. From the same initial condition, the ensemble is integrated with $SGCM_{C8}$ and $SSCM_{C8}$, respectively, without observational constraint. The time

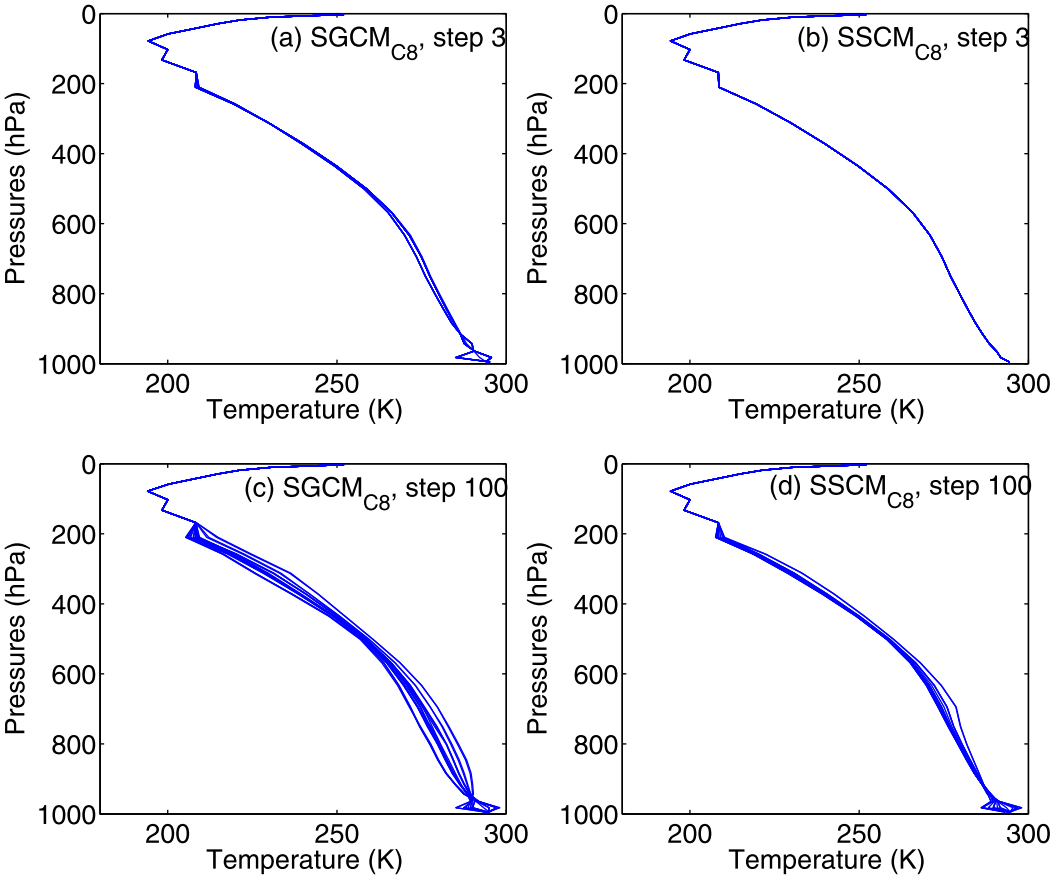

FIG. 7. Time evolution of the temperature profile ensemble of column 8 in SGCM$_{C8}$ and SSCM$_{C8}$. The experiment setting is the same as in Fig. 6c. All ensemble members are integrated from the same initial condition but perturbed parameter α values. (a) The temperature profile ensemble in SGCM$_{C8}$ after the first three steps, during which no convection happens. The ensemble is inflated by 1000 times to make the difference clearer. (b) The temperature profile ensemble in SSCM$_{C8}$ after the first three steps, during which no convection happens. (c),(d) As in (a),(b), but at the 100th time step, before which there are several convective events. The profile ensemble is inflated by 10 times.

evolution of temperature profiles of column 8 is tracked. The initial condition is the same as the line shown in Fig. 7b (the reason will be explained later). During the first three time steps, there is no convection in column 8. Temperature profile ensembles at the third time step in SGCM$_{C8}$ display a distribution (Fig. 7a) similar to that of later time steps (Fig. 7c). This is because, although there is no convection in column 8 during the first three steps, there is convection in other columns. As we have explained earlier, as long as there is convection, the relationship between parameter and model states is established. And this relationship, as a signal for parameter estimation, is transferred to other columns, including column 8, with the help of the large-scale feedback, which is briefly represented by advection in our study. Therefore, when observations of this column are used for parameter estimation, there is still signal in the parameter–state covariance. The parameter estimation with large-scale feedback thus becomes signal dominant even without local convection. On the contrary, in SSCM$_{C8}$, the surrounding model states are prescribed with observations; therefore, the surrounding information is the same for all members. In this case, there is no local convection, which leads to no convective adjustment, and the advection adjustment is the same for all members, so the temperature profiles of column 8 are all the same for all the members (Fig. 7b), leaving a zero parameter–state covariance. Therefore, there is no signal in the parameter estimation at all. This is also why the profiles remain the same as the initial condition. The profile ensemble is also examined at the one-hundreth time step, before which there are several convection occurrences. The temperature ensemble in SGCM (Fig. 7c) displays a relatively larger sensitivity, which indicates stronger model response to this parameter, while that in SSCM (Fig. 7d) displays smaller

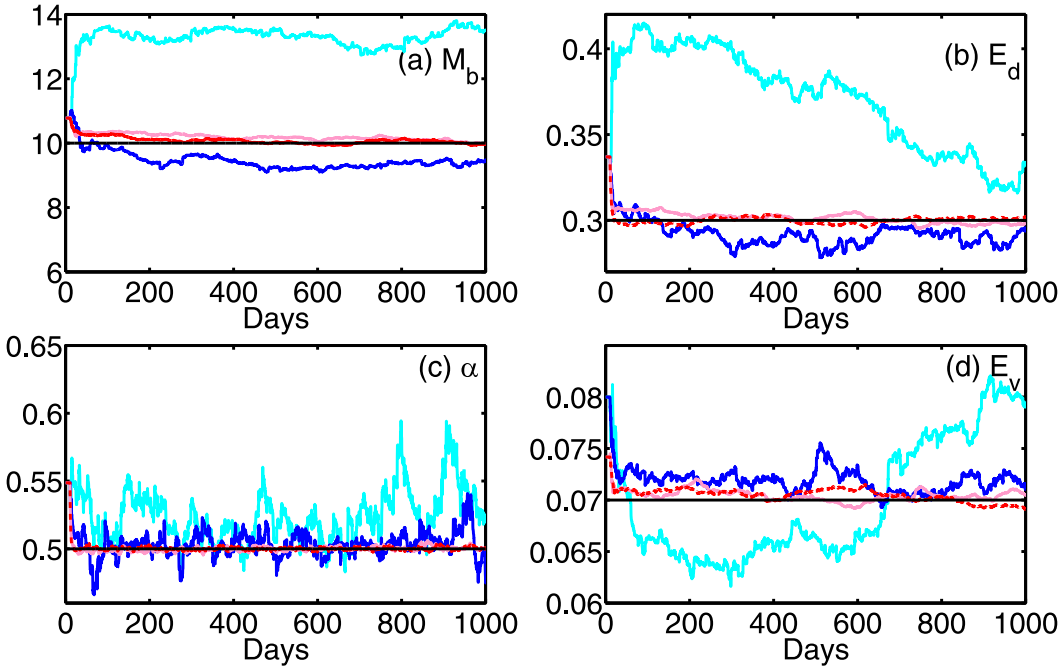

FIG. 8. As in Fig. 5, but for the simultaneous multiple-parameter estimation.

response, indicating a less signal-dominant estimation of the parameter–state relationship. From the above analysis, we can see that, because of the presence of the large-scale feedback, the parameter–state relationship in SGCM is better defined, which consequently leads to a more stable and efficient parameter estimation.

This experiment also indicates that, although in order to estimate cumulus convection parameters, observations of convectively active regions with abundant convection information are more helpful in incorporating more convection signals. With the help of the large-scale feedback, observations of convectively inactive regions can be used to constrain convection parameters. In a GCM, the observations of convectively inactive regions can still be useful because the large scales help transfer the response of the model to the parameter to convectively inactive regions so that the observations without much convection may still be used for estimation of convection parameters. However, the convection frequency in the observations is much more important in an SCM when the large-scale feedback is turned off. Parameter estimation could likely fail if observations of convectively inactive regions are used.

b. *Simultaneous multiple-parameter estimation*

In reality, where the truth parameter values are never known, it is difficult to attribute the model bias to one single parameter. Instead, a set of parameters is usually estimated to help the model best fit observations (Aksoy et al. 2006b; Tong and Xue 2008b; Schirber et al. 2013; Liu et al. 2014a,b). However, because of the compensative effect among multiple parameters (Tong and Xue 2008b; Zhang 2011b), the solution of this optimal set of parameters that minimizes the error from observations may not be unique. And the estimated parameter set that matches the observations quite well may lead to other problems (Golaz et al. 2013). Therefore, it is necessary to examine the ability of one estimation system to find out the true set of parameters under the multiple-parameter estimation setting. The performances of multiple-parameter estimation in SSCM and SGCM are also compared in Fig. 8, with the same observations described in the last section.

1) Regardless of the observation locations, estimations in $SGCM_{C3}$ (red lines) and $SGCM_{C8}$ (pink lines) are generally able to converge to the truth when estimating all parameters simultaneously. And the simultaneous-parameter estimation does not significantly degrade the estimation in the SGCM configuration, which is consistent with the study of Schirber et al. (2013). This is understandable in this case by recognizing the fact that the four parameters have different sensitivities and correlations with state variables. As we have seen from Fig. 6, α is the most sensitive parameter. Also, α has very high correlation with the model temperature (Fig. 9a, dashed–dotted line). At each analysis step, parameter α is first corrected, and the uncertainty of this parameter is greatly

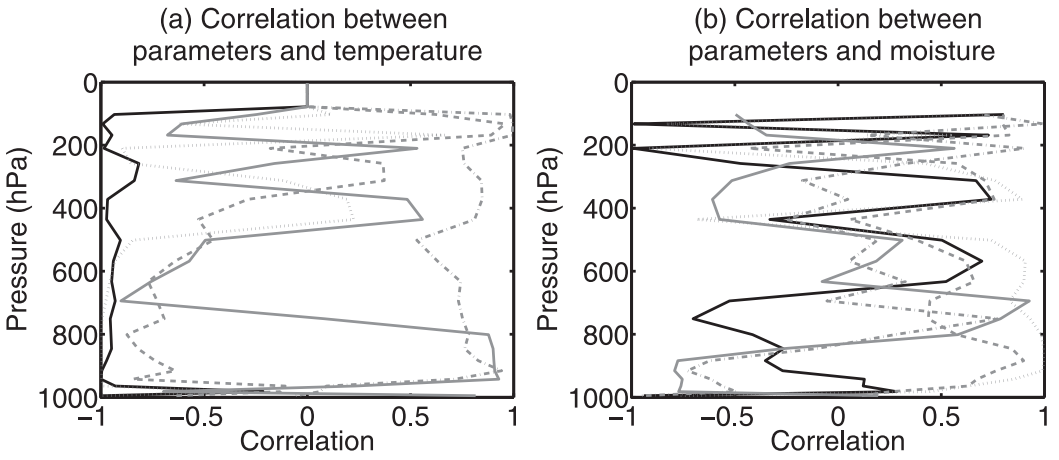

FIG. 9. The correlation between parameter values and state variables: (a) for temperature and (b) for specific humidity. The solid black line corresponds to the radiative cooling rate, and the solid (dashed, dashed–dotted, and dotted) gray lines correspond to M_b (E_d, α, and E_v). This correlation is calculated by perturbing the parameter with 1000 random noises of Gaussian distribution of $N(0, \sigma)$, where σ is 10% of the default value of the parameter, and then running the model for 1000 time steps and calculating the correlation between parameters and state variables.

reduced. After that, the parameter that is the second most sensitive (E_v) and has the second highest correlation (E_v for temperature; Fig. 9a) is corrected, and uncertainty of this parameter is also reduced. This process goes on and on until the least sensitive parameter is corrected. It is noted that, when estimating multiple parameters simultaneously, because of the multimode parameter–model state probability distribution and the compensation effect between parameters, it is possible that other optimal solutions exist other than the truth solution. In our perfect model twin-experiment framework, we assume that the ability to retrieve the truth solution in a certain sense guarantees the ability to retrieve most of the truth model behaviors while helping minimize the analysis error of model states.

2) In this simultaneous-parameter estimation case, the SSCM generates greater error than in the single-parameter estimation experiment, except for α in the SSCM_{C8} (Fig. 8), and it takes much longer for parameters to converge. This is because, when multiple parameters are biased and perturbed, the degree of freedom becomes higher, and the sensitivity of the truth model is increased. But since the sensitivity is underestimated by the SSCM, constraints of the advection from the ''correct'' observation may overwhelm the sensitivity caused by less sensitive parameters. Compensating effect in the moisture between the precipitation efficiency and the evaporation efficiency becomes significant so that for each model configuration the deviations of the estimated parameter value from the truth value for E_d and E_v are opposite.

It is noticed that, in parameter estimation with the SGCM, the compensation effect seems to have little negative influence on estimation results. However, parameter estimation is generally degraded in the SSCM. It is possible that, when the neighboring constraints prevent parameter-induced uncertainty from accumulating, the compensation effect becomes more important so that the estimations for less sensitive parameters are degraded.

5. Parameter estimation in a biased-model context

In reality, there are many parameters related to other physical processes that can significantly influence the model climate and are not corrected. And the climate drift in the GCM is caused not by a single parameter, but by a combination of the effects of all biased parameters. These types of unknown parameter biases can be referred to as ''hidden biases.'' When confronting hidden bias, parameter estimation is carried out under a biased-model context within a biased model in which the compensation effect between different parameter biases exists (Schirber et al. 2013; Tong and Xue 2008b; Aksoy et al. 2006b; Tong and Xue 2008b; Zhang 2011b). Under the influence of compensation, parameter estimation is confronted with mainly two questions. First, with the hidden bias, are we able to find out the truth value of one known erroneously set parameter? This is very difficult but possible if the physical process controlled by this known biased parameter is largely irrelevant to that of the hidden bias. Second, are we able to find the optimal values for one or several parameters

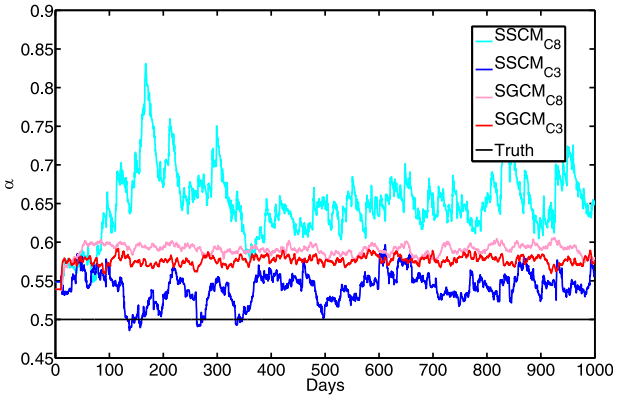

FIG. 10. Single-parameter estimation under the biased-radiation model regime. In this experiment, the biased model is constructed by adding a 10% bias on the radiative cooling rate. Parameter α is used for the single-parameter estimation.

that can compensate for the error caused by the hidden bias? This is more applicable but could be very dangerous because the compensating parameters and the hidden bias may belong to different physical processes. As such, using one to compensate the other may result in serious side effects in other physical quantities that are not considered in the cost function in the parameter estimation. For example, if we tend to minimize the error in temperature and moisture by estimating the cloud parameter to compensate for hidden radiation bias, a large error may emerge in precipitation, and the profiles of the temperature and moisture may become very unrealistic. In our study, we try to estimate cumulus convection parameters with the hidden bias in radiation. The biased model is set by adding a 10% cooling bias to the radiative cooling rate R. A forecast is made with the biased radiative cooling rate and the estimated cumulus convection parameters after the estimations converge. The climatology of state variables (temperature and moisture) is compared with the truth to determine estimation quality.

a. Single-parameter estimation in a biased model

The most sensitive convection parameter, α (see Fig. 6c), is chosen for a single-parameter estimation experiment. The estimation is conducted with the SGCM$_{C3}$, SGCM$_{C8}$, SSCM$_{C3}$, and SSCM$_{C8}$ model configurations to explore the influence of large-scale feedbacks as well as the importance of convection density in observations. The estimated α converges to values different from the truth in different model configurations (Fig. 10). Nevertheless, in all configurations, estimated α values are significantly higher than the truth value of 0.5. This is reasonable because, on one hand, the radiative cooling parameter and α have a strong opposite correlation with modeled temperature (Fig. 9a). In the biased model, when a larger radiative cooling rate is used, the temperature is reduced. To compensate for this cooling effect, larger α should be applied to increase the temperature. Physically, when α is increased, the entrainment rate is reduced (Pan and Wu 1995). By entraining in less cold air from the outside environment and diluting the buoyancy of the cloud, the mixing between the inside cumulus cloud and outside environment is reduced, which helps maintain high temperature in the convection column (Simpson 1971; Rooy et al. 2013). On the other hand, the larger radiative cooling rate bias causes the atmosphere to be more unstable, while the estimated higher α value leads to less entrainment, which results in a more stable atmosphere.

A forecast with the α-optimized, hidden-radiation-bias-presented SGCM is conducted to verify the compensation effect of α to the hidden radiation bias. The comparison of the climatology error (forecast truth) of state variables of the SGCM$_{C3}$, SSCM$_{C3}$, SGCM$_{C8}$, and SSCM$_{C8}$ is shown in Fig. 11. First, the SGCM method gives better climatology than the SSCM, whatever observations are used. This is because, in the SGCM configuration, the relationship between parameters and state variables is fully resolved. Second, the temperature in SGCM$_{C3}$ and SSCM$_{C3}$ has a cold bias, while that in SGCM$_{C8}$ and SSCM$_{C8}$ has a warm bias. Radiation cools the atmosphere, while convection heats the atmosphere. There is more convection around column 3, where convection helps mitigate a large portion of the radiation-bias-induced cooling, thus making the temperature increment $\Delta y^o_{k,i}$ in Eq. (7) smaller when doing data assimilation, which leads to a smaller parameter increment $\Delta\varphi^u_{m,i}$ in Eq. (8). Therefore, α estimated with the SGCM$_{C3}$ and SSCM$_{C3}$ (SGCM$_{C8}$ and SSCM$_{C8}$) is smaller (larger), and the entrainment in the SGCM$_{C3}$ and SSCM$_{C3}$ (SGCM$_{C8}$ and SSCM$_{C8}$) is larger (smaller), which leads to relatively lower (higher) temperature and lower (higher) moisture. With higher values of parameter α, the moisture is increased in all model configurations as a result of less dilution of the dry air through entrainment. However, regardless of the error in temperature and moisture, the precipitation is increased in all estimation schemes (not shown) because the radiative cooling bias leads to a less stable atmosphere.

From the above experiment results, we get a conceptual idea that a single-parameter estimation (chosen from a decent sensitivity study) may compensate, to some extent, the hidden bias in a GCM. It is better to be cautious interpreting the result because the estimated parameter is from different physical processes. The result not only depends on model configurations (SGCM

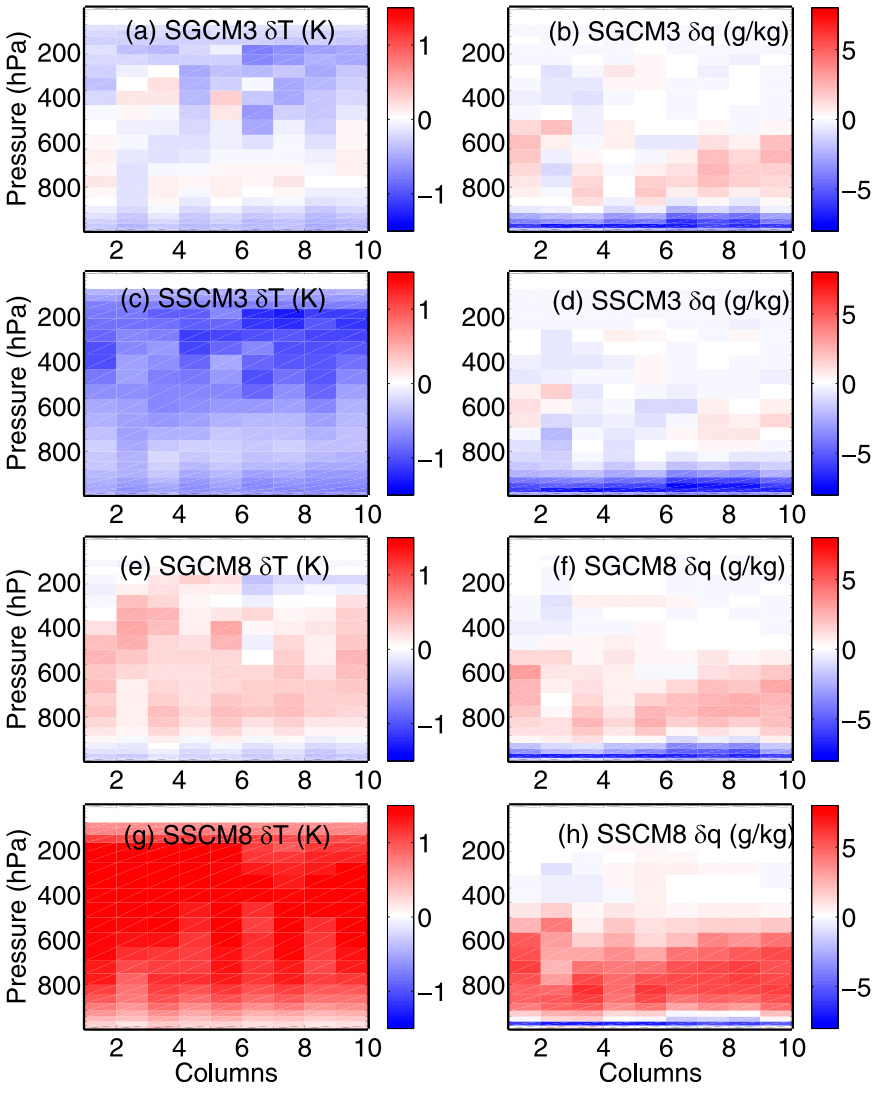

FIG. 11. Forecast climatology error (forecast truth) with estimated parameters in the single-parameter estimation when hidden bias is present. (a),(c),(e),(g) The error of the forecasted temperature climatology from the truth. (b),(d),(f),(h) The error of the forecasted moisture climatology from the truth. The source of the parameter estimation used is the (a),(b) $SGCM_{C3}$, (c),(d) $SSCM_{C3}$, (e),(f) $SGCM_{C8}$, and (g),(h) $SSCM_{C8}$.

or SSCM) and observation locations (columns 2–4 or columns 7–9) but is also closely related to the physical processes. In addition, this compensation could be dangerous because errors may emerge in other quantities that are not considered in the cost function of parameter estimation. Parameter estimation and forecast with a biased model for the other three parameters are less obvious, but with similar mechanism. In more realistic models, this compensation does happen occasionally (Golaz et al. 2013). It might help improve the desired performance but could result in larger bias in other model aspects. This remains a very tough issue in current parameter estimation in various models. And it is also the reason why it is even more difficult to tune model parameters manually.

b. *Simultaneous-parameter estimation in the biased model*

A final experiment is made to find a set of harmonious parameters to compensate for the hidden bias in the biased model. The biased model is the same as that in the single-parameter estimation introduced in the last section. The four suspicious cumulus convection parameters (Table 1) are estimated simultaneously. All four parameters converge to certain values for the $SGCM_{C3}$, $SGCM_{C8}$, and $SSCM_{C3}$ (Fig. 12). For $SSCM_{C8}$, M_b, E_d,

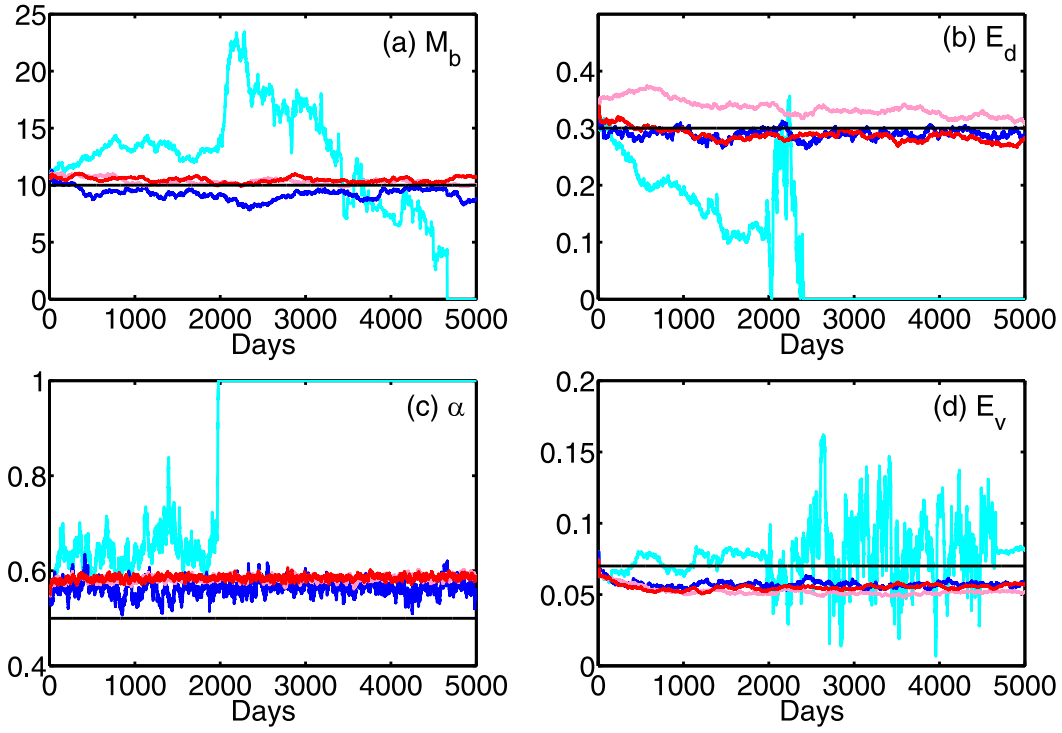

FIG. 12. Simultaneous-parameter estimation of the SSCM and SGCM under the biased model regime. The estimated ensemble mean of the $SGCM_{C3}$ ($SGCM_{C8}$, $SSCM_{C3}$, and $SSCM_{C8}$) is represented by red (pink, blue, and cyan) lines.

and α tend to go beyond the valid range and stay at the boundary after about 2000 days. This is because, in a biased-model context, when we try to use convection parameters to compensate for the hidden radiative bias with the observations of convectively inactive regions, the ensemble-estimated parameter–state error covariance may be contaminated with noises. This is not a big problem for $SGCM_{C8}$ because the large-scale feedback helps transfer the parameter uncertainties from convectively active regions to convectively inactive regions. However, in $SSCM_{C8}$, this large-scale feedback is missing, and the ensemble-estimated covariance becomes more noisy, leaving little signal for parameter estimation. For the $SGCM_{C3}$, $SGCM_{C8}$, and $SSCM_{C3}$, the most significant compensation comes from parameter α, with estimated values higher than those in the perfect model (Fig. 12c) experiment in model configurations of $SGCM_{C3}$, $SGCM_{C8}$, and $SSCM_{C3}$, since α is the most sensitive parameter (Fig. 6c) and has the most robust relationship with temperature (Fig. 9a), as discussed in the previous section. To examine the estimation, forecasts for the $SGCM_{C3}$, $SGCM_{C8}$, and $SSCM_{C3}$ are also made with the converged parameter values. Generally, compared with the single-parameter estimation case, the error of the climatological temperature and moisture is reduced (Fig. 13), except for temperature in the $SSCM_{C3}$ (Fig. 13c). The improvement in moisture is likely due to the inclusion of the moisture-related evaporation parameter E_v, which maintains a high correlation with moisture in the lower atmosphere (Fig. 9b). The cold biases in the $SGCM_{C3}$ and $SSCM_{C3}$ are more obvious, and the warm bias in $SGCM_{C8}$ is less obvious. The estimated α is actually larger (smaller) in the $SSCM_{C3}$ and $SGCM_{C3}$ ($SGCM_{C8}$), indicating that the inclusion of the other three parameters may have a cooling effect on the whole system. In conclusion, finding a set of coherent parameters to compensate for the hidden bias may help improve the overall climatology but remains challenging because of the complexity of the relationship between parameter biases (Posselt and Bishop 2012; Posselt et al. 2014).

6. Conclusions and discussion

A multiple-column atmospheric model is designed that links convective columns together by the advection to form a simplified general circulation model (SGCM). When the feedback between convective columns and large scales is turned off, the model degrades to a simplified single-column model (SSCM). With two model configurations (SGCM and SSCM), the role of large-scale feedbacks on cumulus convection parameter

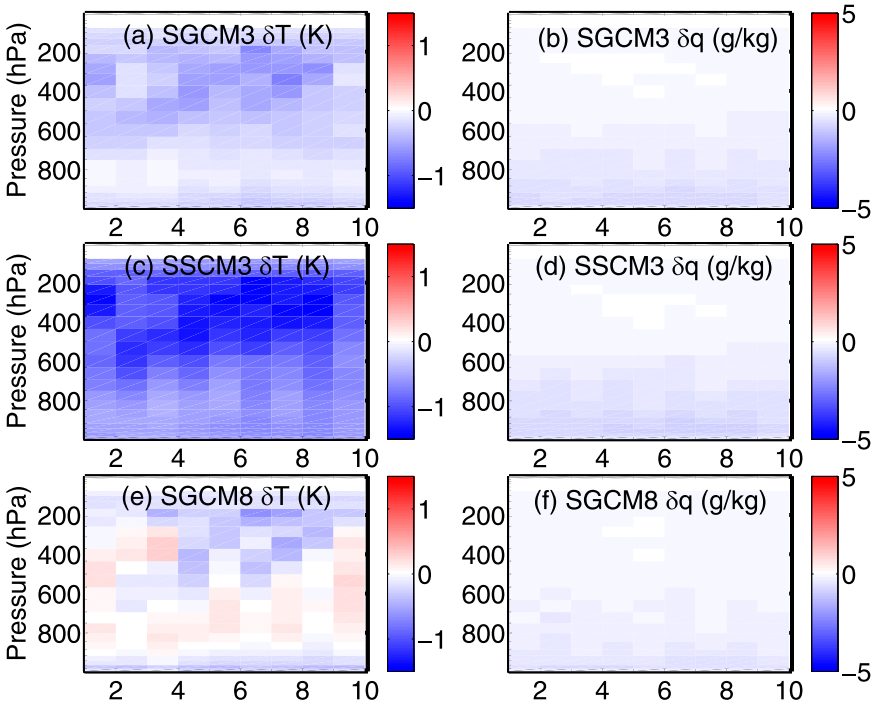

FIG. 13. As in Fig. 11, but for the simultaneous multiple-parameter estimation.

estimation is explored under different practical conditions. We examined the impacts of observational locations (at convectively active and inactive regions), estimation configurations (single- and multiple-parameter estimations), and model error regimes (perfect- and biased-model contexts). Results show that including the large-scale feedback is important in tuning parameters in cumulus convection parameterization for climate modeling because of its role in transferring convection information into large-scale impact. This is realized by enhancing the signal-to-noise ratio in the statistical representation of the relationship between convection parameters and state variables. In ensemble-based parameter estimation, this statistics representation refers to the error covariance represented by the ensemble. This role of large-scale feedbacks could be even more important for more complex and realistic situations.

Robust convection parameter estimation is crucial for improving climate simulation by reducing model biases because it helps improve representation of the physical process and thus reduces model errors. In addition, it is expected that significant climate phenomena, such as ENSO and monsoons, could be better predicted when convection parameters are optimally estimated. With greater efforts to optimize physical parameters in GCMs with the real observing system, climate simulation and prediction is expected to be progressively advanced.

Because of the difficulty in separating local convection and large-scale feedbacks and the challenge of estimating convection parameters in a GCM (Schirber et al. 2013), the simple column-based model with the simplest representation of large-scale feedbacks is first used to explore the influence of the large-scale feedback in estimating convection parameters. Although this preliminary research has provided promising results in cumulus convection parameter estimation, more work needs to be done in the future. Most importantly, more realistic models with more realistic large-scale feedbacks should be involved. The large-scale feedback in this research is simply represented by the temperature and moisture gradients in the advection term. However, in more realistic models, the local convection not only affects other locations through gradients in the advection but also modifies the wind field, radiation, precipitation, and cloud effect, thus influencing the energy budget of the Earth system (Gupta et al. 2013), and changes the pattern of large-scale flows. Besides, in more realistic models, the physical processes would be more complete. For example, the large-scale cloud precipitation and the radiation response to the cloud would be included. With more realistic large-scale feedback and more complete physical processes, the model would have more complex sensitivities to the uncertainty of convection parameters. One would naturally expect a

more important role of large-scale feedbacks in convection parameter estimation.

Second, in this research, to make the large-scale feedback easily turned on or off, the surface pressure, boundary SST, radiative cooling, and wind profiles are fixed. However, in the real world and in more realistic models, these physical quantities are constantly interacting with each other, bringing in more variability and complexity. When more variables and physical processes are included in the model, we would have more options for observation systems. For data assimilation and parameter estimation with real observations, the selection of observations becomes quite important. In the real world, there are not sufficient observations of temperature and moisture profiles, especially in ocean and desert regions. Top-of-the-atmosphere radiative fluxes are potentially a better choice for their wide coverage, high resolution, and frequency. However, recent studies reveal that the relationship between observations and cloud parameters in the convection parameterization scheme is very complicated, so the selection of observations may influence the quality of data assimilation and parameter estimation (Posselt and Vukicevic 2010; Posselt and Bishop 2012; Posselt et al. 2014; van-Lier-Walqui et al. 2012, 2014).

In more realistic models, the influence of the occurrence of convection on parameter estimation may become very important. In our simple model with fixed radiation, wind shear, and boundary heating, the convection occurs very frequently. Therefore, the parameter–state relationship is relatively robust. However, in the real GCM, where the convection is more sparse and rare, the lower occurrence of convection may lead to a seasonal variability of the convergence of the parameter estimation: for summer, when there are more convective events and more convection observations, the estimation could be more signal dominant, whereas for winter the estimation could be more noise dominant. If future study does show such seasonal variability, the role of the large-scale feedback could become more crucial because large-scale feedback helps transfer parameter–state relationships from convectively active regions to other areas and helps preserve the convective signal. However, how much the large-scale would contribute also depends on the complexity and nonlinearity of the large-scale feedback. It is also noted that, although our study showed promising results using observations of convectively inactive regions to estimate parameters in the cumulus convection parameterization schemes in a GCM where large-scale feedbacks are included, given that the parameter would have strong influence on global climatology, it still needs to be tested in more realistic models where more physical processes and complexities are included.

Acknowledgments. This research is sponsored by Chinese MOST 2012CB955200, NSFC41130105, NOAA/GFDL, and China Scholarship Council (awarded to Shan Li for two years' study abroad at NOAA/GFDL). Special thanks go to Drs. Tom Delworth and Gabriel Vecchi at GFDL for their persistent support and generous discussions on this project. We also thank Drs. Monika Barcikowska, Baoqiang Xiang, Yun Liu, and Feiyu Lu and three anonymous reviewers for useful comments.

REFERENCES

Aksoy, A., F. Zhang, and J. W. Nielsen-Gammon, 2006a: Ensemble-based simultaneous state and parameter estimation with MM5. *Geophys. Res. Lett.*, **33**, L12801, doi:10.1029/2006GL026186.

——, ——, and ——, 2006b: Ensemble-based simultaneous state and parameter estimation in a two-dimensional sea-breeze model. *Mon. Wea. Rev.*, **134**, 2951–2970, doi:10.1175/MWR3224.1.

Anderson, J. L., 2001: An ensemble adjustment Kalman filter for data assimilation. *Mon. Wea. Rev.*, **129**, 2884–2903, doi:10.1175/1520-0493(2001)129<2884:AEAKFF>2.0.CO;2.

——, 2003: A local least squares framework for ensemble filtering. *Mon. Wea. Rev.*, **131**, 634–642, doi:10.1175/1520-0493(2003)131<0634:ALLSFF>2.0.CO;2.

——, 2010: A non-Gaussian ensemble filter update for data assimilation. *Mon. Wea. Rev.*, **138**, 4186–4198, doi:10.1175/2010MWR3253.1.

Annan, J. D., and J. C. Hargreaves, 2004: Efficient parameter estimation for a highly chaotic system. *Tellus*, **56A**, 520–526, doi:10.1111/j.1600-0870.2004.00073.x.

——, ——, N. R. Edwards, and R. Marsh, 2005: Parameter estimation in an intermediate complexity earth system model using an ensemble Kalman filter. *Ocean Modell.*, **8**, 135–154, doi:10.1016/j.ocemod.2003.12.004.

Arakawa, A., and W. H. Schubert, 1974: Interaction of a cumulus cloud ensemble with the large-scale environment, Part I. *J. Atmos. Sci.*, **31**, 674–701, doi:10.1175/1520-0469(1974)031<0674:IOACCE>2.0.CO;2.

Asselin, R., 1972: Frequency filter for time integrations. *Mon. Wea. Rev.*, **100**, 487–490, doi:10.1175/1520-0493(1972)100<0487:FFFTI>2.3.CO;2.

Banks, H. T., 1992a: *Control and Estimation in Distributed Parameter Systems.* Frontiers in Applied Mathematics, Vol. 11, SIAM, 227 pp.

——, 1992b: Computational issues in parameter estimation and feedback control problems for partial differential equation systems. *Physica D*, **60**, 226–238, doi:10.1016/0167-2789(92)90239-J.

Betts, A. K., and M. J. Miller, 1986: A new convective adjustment scheme. Part II: Single column tests using GATE wave, BOMEX, ATEX, and Arctic air-mass data sets. *Quart. J. Roy. Meteor. Soc.*, **112**, 693–709, doi:10.1002/qj.49711247308.

Braham, R. R., Jr., 1952: The water and energy budgets of the thunderstorm and their relation to thunderstorm development. *J. Meteor.*, **9**, 227–242, doi:10.1175/1520-0469(1952)009<0227:TWAEBO>2.0.CO;2.

Bretherton, C. S., 2007: Challenges in numerical modeling of tropical circulations. *The Global Circulation of the Atmosphere*, T. Schneider and A. H. Sobel, Eds., Princeton University Press, 302–330.

Emanuel, K. A., and M. Živković-Rothman, 1999: Development and evaluation of a convection scheme for use in climate models. *J. Atmos. Sci.*, **56**, 1766–1782, doi:10.1175/1520-0469(1999)056<1766:DAEOAC>2.0.CO;2.

Fairall, C. W., and E. F. Bradley, 2003: Bulk parameterization of air–sea fluxes: Updates and verification for the COARE algorithm. *J. Climate*, **16**, 571–591, doi:10.1175/1520-0442(2003)016<0571:BPOASF>2.0.CO;2.

——, ——, D. P. Rogers, J. B. Edson, and G. S. Young, 1996: Bulk parameterization of air–sea fluxes in TOGA COARE. *J. Geophys. Res.*, **101**, 3747–3767, doi:10.1029/95JC03205.

Golaz, J.-C., V. E. Larson, J. A. Hansen, D. P. Schanen, and B. M. Griffin, 2007: Elucidating model inadequacies in a cloud parameterization by use of an ensemble-based calibration framework. *Mon. Wea. Rev.*, **135**, 4077–4096, doi:10.1175/2007MWR2008.1.

——, L. W. Horowitz, and H. Levy II, 2013: Cloud tuning in a coupled climate model: Impact on 20th century warming. *Geophys. Res. Lett.*, **40**, 2246–2251, doi:10.1002/grl.50232.

Grell, G. A., 1993: Prognostic evaluation of assumptions used by cumulus parameterization. *Mon. Wea. Rev.*, **121**, 764–787, doi:10.1175/1520-0493(1993)121<0764:PEOAUB>2.0.CO;2.

Guichard, F., and Coauthors, 2004: Modelling the diurnal cycle of deep precipitating convection over land with cloud-resolving models and single-column models. *Quart. J. Roy. Meteor. Soc.*, **130**, 3139–3172, doi:10.1256/qj.03.145.

Gupta, A. S., N. C. Jourdain, J. N. Brown, and D. Monselesan, 2013: Climate drift in the CMIP5 models. *J. Climate*, **26**, 8597–8615, doi:10.1175/JCLI-D-12-00521.1.

Hourdin, F., and Coauthors, 2006: The LMDZ4 general circulation model: Climate performance and sensitivity to parametrized physics with emphasis on tropical convection. *Climate Dyn.*, **27**, 787–813, doi:10.1007/s00382-006-0158-0.

Hu, X. M., F. Zhang, and J. W. Nielsen-Gammon, 2010: Ensemble-based simultaneous state and parameter estimation for treatment of mesoscale model error: A real-data study. *Geophys. Res. Lett.*, **37**, L08802, doi:10.1029/2010GL043017.

Jazwinski, A. H., 1970: *Stochastic and Filtering Theory*. Mathematics in Science and Engineering, Vol. 64, Academic Press, 376 pp.

Kang, J. S., E. Kalnay, J. Liu, I. Fung, T. Miyoshi, and K. Ide, 2011: "Variable localization" in an ensemble Kalman filter: Application to the carbon cycle data assimilation. *J. Geophys. Res.*, **116**, D09110, doi:10.1029/2010JD014673.

Klocke, D., R. Pincus, and J. Quaas, 2011: On constraining estimates of climate sensitivity with present-day observations through model weighting. *J. Climate*, **24**, 6092–6099, doi:10.1175/2011JCLI4193.1.

Knight, C. G., and Coauthors, 2007: Association of parameter, software, and hardware variation with large-scale behavior across 57,000 climate models. *Proc. Natl. Acad. Sci. USA*, **104**, 12 259–12 264, doi:10.1073/pnas.0608144104.

Lau, K., and P. H. Chan, 1988: Intraseasonal and interannual variations of tropical convection: A possible link between the 40–50 day oscillation and ENSO? *J. Atmos. Sci.*, **45**, 506–521, doi:10.1175/1520-0469(1988)045<0506:IAIVOT>2.0.CO;2.

Lin, J.-L., and Coauthors, 2006: Tropical intraseasonal variability in 14 IPCC AR4 climate models. Part I: Convective signals. *J. Climate*, **19**, 2665–2690, doi:10.1175/JCLI3735.1.

Liu, W. T., K. B. Katsaros, and J. A. Businger, 1979: Bulk parameterization of air–sea exchanges of heat and water vapor including the molecular constraints at the interface. *J. Atmos. Sci.*, **36**, 1722–1735, doi:10.1175/1520-0469(1979)036<1722:BPOASE>2.0.CO;2.

Liu, Y., Z. Liu, S. Zhang, R. Jacob, F. Lu, X. Rong, and S. Wu, 2014a: Ensemble-based parameter estimation in a coupled general circulation mode. *J. Climate*, **27**, 7151–7162, doi:10.1175/JCLI-D-13-00406.1.

——, ——, ——, X. Rong, R. Jacob, S. Wu, and F. Lu, 2014b: Ensemble-based parameter estimation in a coupled GCM using the adaptive spatial average method. *J. Climate*, **27**, 4002–4014, doi:10.1175/JCLI-D-13-00091.1.

Lord, S., 1982: Interaction of a cumulus cloud ensemble with the large-scale environment. Part III: Semi-prognostic test of the Arakawa–Schubert cumulus parameterization. *J. Atmos. Sci.*, **39**, 88–103, doi:10.1175/1520-0469(1982)039<0088:IOACCE>2.0.CO;2.

——, and A. Arakawa, 1980: Interaction of a cumulus cloud ensemble with the large-scale environment. Part II. *J. Atmos. Sci.*, **37**, 2677–2692, doi:10.1175/1520-0469(1980)037<2677:IOACCE>2.0.CO;2.

Ma, H. Y., S. Xie, J. S. Boyle, S. A. Klein, and Y. Zhang, 2013: Metrics and diagnostics for precipitation-related processes in climate model short-range hindcasts. *J. Climate*, **26**, 1516–1534, doi:10.1175/JCLI-D-12-00235.1.

Mrowiec, A. A., C. Rio, A. M. Fridlind, A. S. Ackerman, A. D. Del Genio, O. M. Pauluis, A. C. Varble, and J. Fan, 2012: Analysis of cloud-resolving simulations of a tropical mesoscale convective system observed during TWP-ICE: Vertical fluxes and draft properties in convective and stratiform regions. *J. Geophys. Res.*, **117**, D19201, doi:10.1029/2012JD017759.

Mukhopadhyay, P., S. Staraphdar, B. N. Coswami, and K. Krishnakumar, 2010: Indian summer monsoon precipitation climatology in a high-resolution regional climate model: Impacts of convective parameterization on systematic biases. *Wea. Forecasting*, **25**, 369–387, doi:10.1175/2009WAF2222320.1.

Murphy, J. M., D. M. H. Sexton, D. N. Barnett, G. S. Jones, M. J. Webb, M. Collins, and D. A. Stainforth, 2004: Quantification of modelling uncertainties in a large ensemble of climate change simulations. *Nature*, **430**, 768–772, doi:10.1038/nature02771.

Pan, H., and W. Wu, 1995: Implementing a mass flux convection parameterization package for the NMC Medium-Range Forecast model. NCEP Office Note 409, 43 pp. [Available online at http://www.emc.ncep.noaa.gov/officenotes/FullTOC.html.]

Park, A., and W. Funk, 2011: A westward extension of the warm pool leads to a westward extension of the Walker circulation, drying eastern Africa. *Climate Dyn.*, **37**, 2417–2435, doi:10.1007/s00382-010-0984-y.

Posselt, D. J., and T. Vukicevic, 2010: Robust characterization of model physics uncertainty for simulations of deep moist convection. *Mon. Wea. Rev.*, **138**, 1513–1535, doi:10.1175/2009MWR3094.1.

——, and C. H. Bishop, 2012: Nonlinear parameter estimation: Comparison of an ensemble Kalman smoother with a Markov chain Monte Carlo algorithm. *Mon. Wea. Rev.*, **140**, 1957–1974, doi:10.1175/MWR-D-11-00242.1.

——, D. Hodyss, and C. H. Bishop, 2014: Errors in ensemble Kalman smoother estimates of cloud microphysical

parameters. *Mon. Wea. Rev.*, **142**, 1631–1654, doi:10.1175/MWR-D-13-00290.1.

Pulido, M., and J. Thuburn, 2006: Gravity wave drag estimation from global analyses using variational data assimilation principles. Part II: A case study. *Quart. J. Roy. Meteor. Soc.*, **132**, 1527–1543, doi:10.1256/qj.05.43.

Randall, D. A., K. Xu, R. J. C. Somerville, and S. Iacobellis, 1996: Single-column models and cloud ensemble models as links between observations and climate models. *J. Climate*, **9**, 1683–1697, doi:10.1175/1520-0442(1996)009<1683:SCMACE>2.0.CO;2.

Rennó, N. O., K. A. Emanuel, and P. H. Stone, 1994: Radiative-convective model with an explicit hydrologic cycle: 1. Formulation and sensitivity to model parameters. *J. Geophys. Res.*, **99**, 14 429–14 441, doi:10.1029/94JD00020.

Rooy, W. C., and Coauthors, 2013: Entrainment and detrainment in cumulus convection: An overview. *Quart. J. Roy. Meteor. Soc.*, **139**, 1–19, doi:10.1002/qj.1959.

Rougier, J., D. M. H. Sexton, J. M. Murphy, and D. Stainforth, 2009: Analyzing the climate sensitivity of the HadSM3 climate model using ensembles from different but related experiments. *J. Climate*, **22**, 3540–3557, doi:10.1175/2008JCLI2533.1.

Ruiz, J., and M. Pulido, 2014: Parameter estimation using ensemble-based data assimilation in the presence of model error. *Mon. Wea. Rev.*, **143**, 1568–1582, doi:10.1175/MWR-D-14-00017.1.

——, ——, and T. Miyoshi, 2013: Estimating model parameters with ensemble-based data assimilation: A review. *J. Meteor. Soc. Japan*, **91**, 79–99, doi:10.2151/jmsj.2013-201.

Schirber, S., D. Klocke, R. Pincus, J. Quaas, and J. L. Anderson, 2013: Parameter estimation using data assimilation in an atmospheric general circulation model: From a perfect toward the real world. *J. Adv. Model. Earth Syst*, **5**, 58–70, doi:10.1029/2012MS000167.

Simpson, J., 1971: On cumulus entrainment and one-dimensional models. *J. Atmos. Sci.*, **28**, 449–455, doi:10.1175/1520-0469(1971)028<0449:OCEAOD>2.0.CO;2.

Sobel, A., and G. Bellon, 2009: The effect of imposed drying on parameterized deep convection. *J. Atmos. Sci.*, **66**, 2085–2096, doi:10.1175/2008JAS2926.1.

Song, X., and G. J. Zhang, 2009: Convection parameterization, tropical Pacific double ITCZ, and upper-ocean biases in the NCAR CCSM3. Part I: Climatology and atmospheric feedback. *J. Climate*, **22**, 4299–4315, doi:10.1175/2009JCLI2642.1.

Sui, C. H., X. Li, and M. J. Yang, 2007: On the definition of precipitation efficiency. *J. Atmos. Sci.*, **64**, 4506–4513, doi:10.1175/2007JAS2332.1.

Tiedtke, M. A., 1989: Comprehensive mass flux scheme for cumulus parameterization in large-scale models. *Mon. Wea. Rev.*, **117**, 1779–1800, doi:10.1175/1520-0493(1989)117<1779:ACMFSF>2.0.CO;2.

Tokioka, T., K. Yamazaki, A. Kitoh, and T. Ose, 1988: The equatorial 30–60 day oscillation and the Arakawa–Schubert penetrative cumulus parameterization. *J. Meteor. Soc. Japan*, **66**, 883–901.

Tong, M., and M. Xue, 2008a: Simultaneous estimation of microphysical parameters and atmospheric state with simulated radar data and ensemble square root Kalman filter. Part I: Sensitivity analysis and parameter identifiability. *Mon. Wea. Rev.*, **136**, 1630–1648, doi:10.1175/2007MWR2070.1.

——, and ——, 2008b: Simultaneous estimation of microphysical parameters and atmospheric state with simulated radar data and ensemble square root Kalman filter. Part II: Parameter estimation experiments. *Mon. Wea. Rev.*, **136**, 1649–1668, doi:10.1175/2007MWR2071.1.

Tracton, M. S., 1973: The role of cumulus convection in the development of extratropical cyclones. *Mon. Wea. Rev.*, **101**, 573–593, doi:10.1175/1520-0493(1973)101<0573:TROCCI>2.3.CO;2.

van Lier-Walqui, M., T. Vukicevic, and D. J. Posselt, 2012: Quantification of cloud microphysical parameterization uncertainty using radar reflectivity. *Mon. Wea. Rev.*, **140**, 3442–3466, doi:10.1175/MWR-D-11-00216.1.

——, ——, and ——, 2014: Linearization of microphysical parameterization uncertainty using multiplicative process perturbation parameters. *Mon. Wea. Rev.*, **142**, 401–413, doi:10.1175/MWR-D-13-00076.1.

Webster, P. J., and S. Yang, 1992: Monsoon and ENSO: Selectively interactive systems. *Quart. J. Roy. Meteor. Soc.*, **118**, 877–926, doi:10.1002/qj.49711850705.

Wu, X., S. Zhang, Z. Liu, A. Rosati, and T. L. Delworth, 2013: A study of impact of the geographic dependence of observing system on parameter estimation with an intermediate coupled model. *Climate Dyn.*, **40**, 1789–1798, doi:10.1007/s00382-012-1385-1.

Xiang, B., B. Wang, and T. Li, 2013: A new paradigm for the predominance of standing Central Pacific Warming after the late 1990s. *Climate Dyn.*, **41**, 327–340, doi:10.1007/s00382-012-1427-8.

Zhang, S., 2011a: Impact of observation-optimized model parameters on decadal predictions: Simulation with a simple pycnocline prediction model. *Geophys. Res. Lett.*, **38**, L02702, doi:10.1029/2010GL046133.

——, 2011b: A study of impacts of coupled model initial shocks and state–parameter optimization on climate predictions using a simple pycnocline prediction model. *J. Climate*, **24**, 6210–6226, doi:10.1175/JCLI-D-10-05003.1.

——, and J. L. Anderson, 2003: Impact of spatially and temporally varying estimates of error covariance on assimilation in a simple atmospheric model. *Tellus*, **55A**, 126–147, doi:10.1034/j.1600-0870.2003.00010.x.

——, X. Zou, and J. E. Ahlquist, 2001: Examination of numerical results from tangent linear and adjoint of discontinuous nonlinear models. *Mon. Wea. Rev.*, **129**, 2791–2804, doi:10.1175/1520-0493(2001)129<2791:EONRFT>2.0.CO;2.

——, M. J. Harrison, A. Rosati, and A. T. Wittenberg, 2007: System design and evaluation of coupled ensemble data assimilation for global oceanic climate studies. *Mon. Wea. Rev.*, **135**, 3541–3564, doi:10.1175/MWR3466.1.

——, Z. Liu, A. Rosati, and T. Delworth, 2012: A study of enhancive parameter correction with coupled data assimilation for climate estimation and prediction using a simple coupled model. *Tellus*, **64A**, 10963, doi:10.3402/tellusa.v64i0.10963.

Zhang, X.-F., S. Zhang, Z. Liu, X. Wu, and G. Han, 2015: Parameter optimization in an intermediate coupled climate model with biased physics. *J. Climate*, **28**, 1227–1247, doi:10.1175/JCLI-D-14-00348.1.

Županski, D., 1993: The effects of discontinuities in the Betts–Miller cumulus convection scheme on four-dimensional variational data assimilation. *Tellus*, **45A**, 511–524, doi:10.1034/j.1600-0870.1993.00013.x.